Arbitrary Strain and Temperature Distribution Sensing Using Two FBG Pairs

[a]Hsu-Chih Cheng and [b]Yu-Lung Lo
[a]Department of Computer and Communication, Diwan University, Tainan, Taiwan
*[b]Department of Mechanical Engineering, National Cheng Kung University,
No.1, Ta-Hsueh Road, Tainan 701, Taiwan ROC
*Correspond author: loyl@mail.ncku.edu.tw

ABSTRACT

We use two pairs of FBGs to perform simultaneous strain and temperature field measurements. The first pair of FBGs, comprising one uniform FBG and one chirped FBG, measures the strain and temperature fields, while the second pair of FBGs, also comprising one uniform FBG and one chirped FBG, measures the temperature field only. A genetic algorithm is applied to reconstruct the arbitrary strain and temperature distribution profiles simultaneously from the measured reflection intensity spectra of the four FBGs. Also, we include the reflection power attenuation factors into the genetic algorithm and make this approach more useful in practical. Several strain distributions along the fiber Bragg gratings are reconstructed numerically. The proposed measurement method is suitable for many smart structure-monitoring applications.

1. Introduction

Fiber optic sensors exploit the fact that light guided within an optical fiber can be modified by external physical, chemical, biomedical, biological, or similar influences. Fiber optic sensors have many advantages, chief of which are their light weight, small size, high sensitivity, immunity to electromagnetic interference, large bandwidth, and ease of implementation as multiplexing or distributed sensors. In the recent years, many temperature and strain distribution sensing techniques that using FBGs were presented sequentially. Those methods have been developed quite successfully [1-12]. Huang et al. [1-3] presented a series of articles relating to FBGs strain distribution sensing using either the intensity spectrum or the phase spectrum, or a combination of both. They used the intensity-spectra-based and phase-spectra-based method to inversely track the distributed strain profile [1, 2]. However, intensity-spectra-based [1] and phase-spectra-based [2] inverse methods are applicable only to the cases of monotonically increasing or decreasing period distributions. Huang et al. [3] also developed a Fourier transform method for the synthesis of non-monotonic FBG structures. This method had the advantage of a rapid reconstruction time, but was applicable only to weak FBGs and involved the use of a complex spectrum (i.e. the intensity and phase spectra). Reconstructing the properties of an FBG requires that its complex reflection coefficient be known. In the authors' experience, measuring the phase spectra of a FBG experimentally is difficult and expensive.

The similar methods which use complex reflection coefficient (intensity and phase spectra) to recovery the FBG's properties had been proposed in several articles [4, 5]. The use of a layer-peeling method has been proposed for reconstructing FBG's period distribution [4]. Azana et al. [5] presented a time-frequency signal analysis technique to reconstruct FBG's period distribution and application to distributed sensing. Both methods involved the use of rapid and accurate inverse algorithms but have the drawbacks for complex reflection spectra measuring of FBG. Recently, there are several articles that described the FBG's period reconstruction by using optimization methods such as simulated annealing algorithm, least square, and genetic

algorithm. The simulated annealing and adaptive simulated annealing algorithms can be used for parameter synthesis and distributed strain sensing of FBGs [6, 7]. However, these methods are only suitable when the inverse analysis involves a small number of parameters since they tend to become slower and more inaccurate when the number of parameters increases. Won et al. [8] used one chirped FBG based on the Fabry-Perot effect of FBG to reconstruct the fully temperature distribution along the FBG by using least square fit method. This method is also suitable for monotonic temperature change along the FBG. In genetic algorithm, Skaar and Risvik [9] proposed the use of genetic algorithms for the synthesis of FBGs. They employed a binary genetic algorithm to design a FBG filter for optical communication applications. Casagrande et al. [10] proposed the inverse measurement of distributed strain via the application of a genetic algorithm to the intensity spectrum of the FBG. However, this technique is valid only for monotonic strain profiles. More recently still, Cheng and Lo [11] proposed a novel method to recover the period distribution of an FBG for arbitrary distributed strain sensing applications. This method used a uniform FBG and a chirped FBG to generate two strain-induced reflection intensity spectra only, from which the arbitrary strain distribution along the two parallel FBGs was subsequently reconstructed with genetic algorithm. Cheng and Lo [12] also used the two thermally modulated intensity spectra and genetic algorithm to find the multiple FBG's parameters such as grating period, length, position, chirped direction, and refractive index modulation.

In this paper, we extended the main principle of the previous papers [11, 12] to achieve simultaneously temperature and strain distribution sensing applications. A new approach to easily solve the problems of non-monotonic temperature and strain distribution sensing in fiber optic measurement system is proposed. As the authors' knowledge, no one proposes a method to simultaneously measure the arbitrary temperature and strain fields on the structures by using FBGs. This new approach is based on the genetic algorithm by employing the population-based optimization processes in four reflection intensity spectra of FBGs for inversely tracking the temperature and strain distribution onto FBGs. The basic assumption of this approach is that two pairs of intra-core FBGs are encountering the same temperature field and one of pair encountering the same strain field. As a result, this approach has several advantages such as no limitation in reflectivity like [1-5], only intensity spectra applied in an inverse extraction, and arbitrary temperature and strain field measurements. Also, in the practical application, the power attenuation induced by connector insertion loss and etc is an important issue for discussing. In this paper, we include the power attenuation factor into our presented approach.

The remainder of this paper is organized as follows. Section 2 introduces the basic concepts of the proposed strain and temperature distribution sensing method using two FBGs pair and genetic algorithm. Section 3 presents the current numerical simulation results. Finally, Section 4 summarizes the principal conclusions of the present study.

2. Methodology and Implementation

The schematic diagram of the new measurement system is illustrated in Fig. 1. In our design, we connect a FBG pair (one is uniform FBG and the other chirped FBG) with one output port of a 2x2 coupler and glue them on a substrate in parallel. Another output port of a 2x2 coupler is connected to another FBG pair. If the two FBGs which glued on the substrate are close enough, the strain distribution onto the two FBGs can be assumed the same. Similarly, if all four FBGs are close enough, the temperature field onto the four FBGs can be also assumed the same. According to the above mentions, we can get four different reflection intensity spectra from two FBG pairs and combine genetic algorithm to inversely obtain the arbitrary temperature and strain distributions in the measuring field.

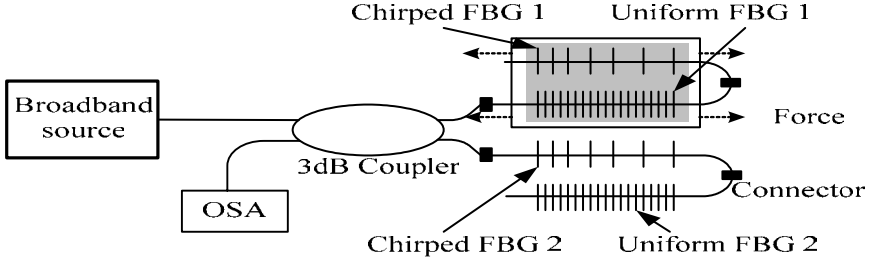

Figure 1 The schematic diagram of temperature and strain distribution sensing application

Genetic algorithms provide an efficient procedure for solving inverse problems. However, before the genetic algorithm can be applied, its solution must be appropriately encoded. In the present case, the genetic algorithm yields the strain and temperature distributions along the FBGs. In a direct analogy to that of genes in the natural biology field, the solutions of the distributed strain field, S(z), and temperature field, T(z), are encoded as a string of real values, as shown in Fig. 6. This approach has the advantage that discontinuous, nonlinear

strain and temperature distributions can be easily represented. In practical, the power attenuation is a problem for strain distribution reconstruction. Hence, we also include four power attenuation factors into the sample string.

S(1)	S(2)	...	...	S(M)	Att. 1	Att. 2

T(1)	T(2)	...	...	T(M)	Att. 3	Att. 4

Figure 2. Sample string of real values

The main effect of the spatial variation of grating period profile Λ(z) and effective refractive index profile n(z) is that each section of the grating mainly contributes to the reflection spectrum at the wavelength of its local Bragg tuning:

$$\Delta\lambda_B = 2n_0\Lambda_0\left(\left\{1-(\frac{n_0^2}{2})[P_{12}-\nu(P_{11}+P_{12})]\right\}S(z)+[\alpha+\xi]T(z)\right) \quad (1)$$

where n0 is the original effective refractive index of the fiber, Λ_0 is the normal grating period, P_{11} and P_{12} are the Pockel's coefficient; ν is Pisson's ratio, α and ξ are the coefficient of thermal expansion of the fiber material (0.55×10^{-6}) and the thermo-optic coefficient at room temperature (6.67×10^{-6}), S(z) is the strain profile and T(z) is the temperature profile along the fiber grating. In most applications in sensing, the temperature and strain along a fiber grating is uniform, and the temperature and strain are determined from the reflective wavelength of the grating. However, if the grating is subjected to the temperature and strain gradient, its reflective spectrum will not only be shifted but also be distorted because of non-uniform changes in both the physical pitch length and the refractive index of the grating. Gratings with non-uniform pitch length, refractive index modulation depth, and mean refractive index of the core have been analyzed in different ways. We use the T-matrix formalism [13], which offers a straightforward way to analyze the reflection spectrum response of non-uniform grating structures. To use the T-matrix modal, we can simulate the FBG's reflection intensity spectrum under non-uniform temperature and strain distribution.

Genetic algorithm is an iterative procedure that represents its candidate solutions as strings of genes called chromosomes and measures their viability with a fitness function. The fitness function (error function) is a measure of the objective to be obtained. As in biological systems, candidate solutions combine to produce offspring in each algorithmic iteration called generation. The offspring themselves can become candidate solutions. From the generation of parents and children, a set of the fittest survives to become parents that produce offspring in next generation [14]. In the genetic algorithm, the error function (fitness function) is a measurement of the distance between the calculated reflection spectra and the target reflection spectra. In this methodology, we have two objective reflection spectra, one of them is due to uniform FBG 1 and a chirped FBG 1 under the temperature and strain profile and another is uniform FBG 2 and a chirped FBG 2 under the same temperature profile only. It tells the genetic algorithm how to select the better solution. Here we define the error function to be

$$Error1 = \sum_{\lambda}(R_{U1,Obj} - Att.1\times R_{U1,Cal})^2 + \sum_{\lambda}(R_{C1,Obj} - Att.2\times R_{C1,Cal})^2 \quad (2)$$

$$Error2 = \sum_{\lambda}(R_{U2,Obj} - Att.3\times R_{U2,Cal})^2 + \sum_{\lambda}(R_{C2,Obj} - Att.4\times R_{C2,Cal})^2 \quad (3)$$

where $R_{U1,Obj}$ and $R_{C1,Obj}$ are mean first uniform and chirped FBG's reflection intensity spectra under a arbitrary temperature and strain distribution. $R_{U2,Obj}$ and $R_{C2,Obj}$ are the second uniform reflective spectrum under a arbitrary temperature distribution. They can be obtained from the optical spectrum analyzer. However, $R_{U1,Cal}$, $R_{U2,Cal}$, $R_{C1,Cal}$, and $R_{C2,Cal}$ are the reflection intensity spectra from the T-matrix analysis method. The objective of the inverse problem is to find a temperature and strain distribution that produced four reflective spectra as close as possible to the target spectra. Att. 1, Att. 2, Att. 3 and Att. 4 are the reflection power attenuation factors, respectively. The objective of the inverse problem is to inversely derive the strain and temperature distribution

which yields the four reflection intensity spectra most closely resembling the target spectra.

There are several steps of this optimization produces, as represented in Fig. 3. At the start of optimization, a genetic algorithm requires a group of initial solutions. First we make some solutions (temperature and strain distributions) randomly to calculate reflection intensity spectra. Second, fixed a sub-optimal temperature profile T(z) and calculating the reflection intensity spectra from these solutions (fixed T(z) and random S(z)) by using T-matrix analysis method and substitute them into Eq. (2) to calculate the error value. Third, we execute genetic algorithm's operators until 100 iterations (selection, crossover and mutation) are achieved. We can obtain the sub-optimal solution of strain profile in this step. Fourth, fix a sub-optimal strain profile S(z) from last step and calculating the reflection intensity spectra from these solutions (random T(z) and fixed S(z)) by using T-matrix analysis method and substitute them into Eq. (3) to calculate the error value too. Also, we execute genetic algorithm's operators until 100 iterations are achieved and find the sub-optimal temperature profile in this step. Finally, we terminate the program until the all error value is less than a small value or the execute loops (5000) is finished.

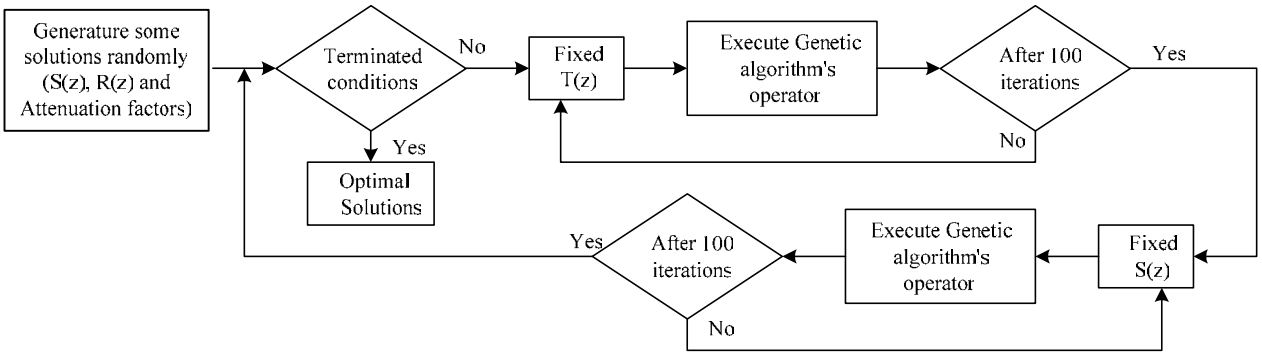

Figure 3 Flow chart of genetic algorithm

3. Numerical results

In the present simulations, the grating length was set to L = 2 cm and was divided into 20 uniform sections. Accordingly, the spatial resolution in the longitudinal direction of the grating was 1 mm. The effective refractive index of the fiber core was assumed to be n_{eff}=1.457, the first and second uniform grating periods were assumed to be Λ_{01U} =528.5 nm and $_{\Lambda 02U}$ =531.8 nm, respectively, and the first and second chirped FBG grating periods were assumed to be Λ_{01C} =530.0 nm and Λ_{02C}=533.45 μm, respectively. Furthermore, the variations in the first and second chirped FBG periods along the grating length were assumed to be $\Lambda_{1C(z)}=\Lambda_{01C}(1+0.0003z)$ and $\Lambda_{2C(z)}=\Lambda_{02C}(1+0.0003z)$, respectively. As discussed previously, the first FBG pair was designed to sense both the arbitrary strain profile and the arbitrary temperature profile, while the second FBG pair was designed to sense only the arbitrary temperature profile. In the current application, the genetic algorithm generates two solutions, namely the strain profile and the temperature profile. The reflection spectra of the FBGs are affected by both profiles. The attenuation factors are also included

Figure 4 presents the reflection intensity spectra of the four fiber Bragg gratings and figure 5 presents the reflection power attenuation due to the attenuation factors. We use the attenuated reflection power into the genetic algorithm and reconstruct the strain distribution and attenuation factor.

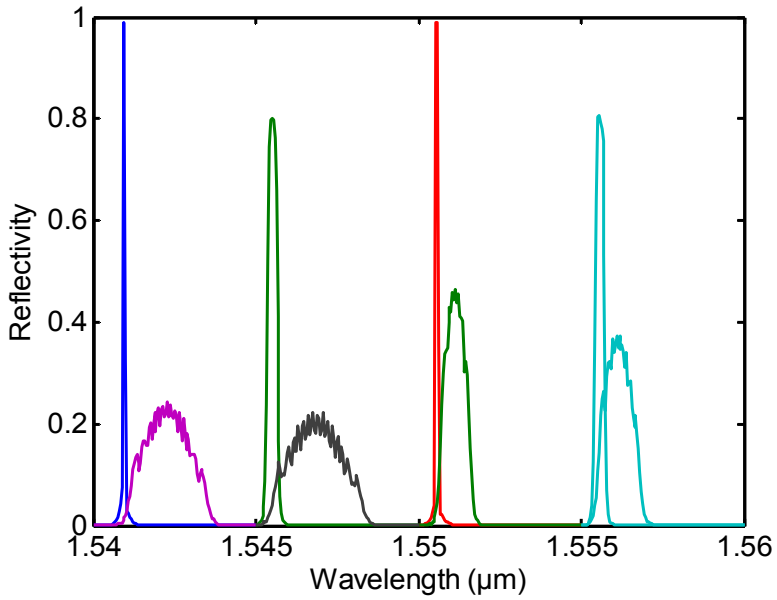

Figure 4 The reflection intensity spectra of the four fiber Bragg gratings.

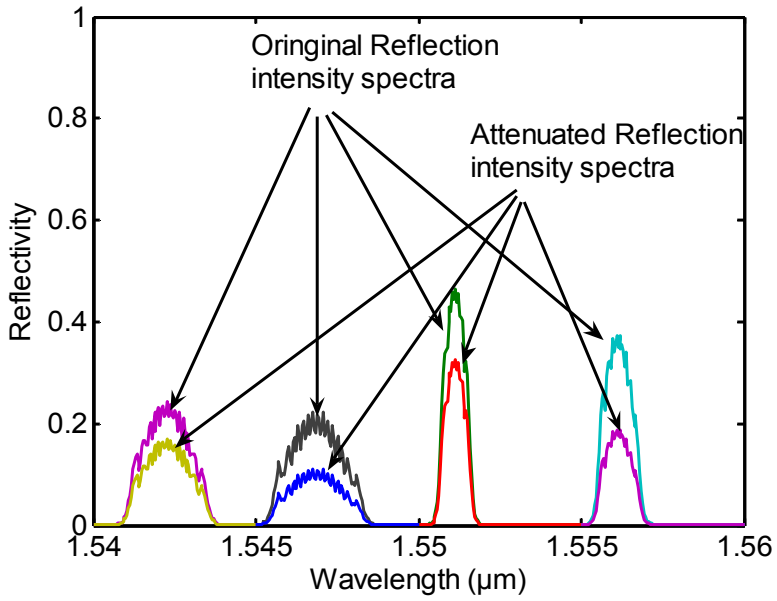

Figure 5 The reflection intensity spectra of the four fiber Bragg grating due to linear gradient strain distribution and the same reflection power attenuation factor (Att.1=Att.3=70%, Att.2=Att.4=50%)

The first simulation case is shown in Fig. 6 and involves a positive linear strain distribution (solid curve) and a positive linear temperature distribution (solid curve), as shown in Figs. 6(a) and 6(b), respectively. The setting attenuation factors are Att.1=0.7, Att.2=0.5, Att.3=0.7, and Att.4=0.5, respectively. Applying these strain and temperature profiles to the four FBGs, the T-matrix method is used to generate the corresponding ideal attenuated reflection intensity spectra (solid curve) shown in Fig. 6(c). The genetic algorithm is then used to derive the arbitrary distributed strain and temperature profiles corresponding to these intensity spectra. The results for the positive linear strain profile (dotted curve) and positive linear temperature profile (dotted curve) are shown in Figs. 6(a) and 6(b), respectively. The corresponding reflection intensity spectra reconstructed by the T-matrix method for the strain and temperature distributions are shown by the dotted curve in Fig. 6(c) and are seen to be in good agreement with the ideal attenuated reflection intensity spectra (solid curve). Also, the reconstructed attenuation factors are Att.1=0.7001, Att.2=0.4992, Att.3=0.7023, and Att.4=0.5031, respectively.

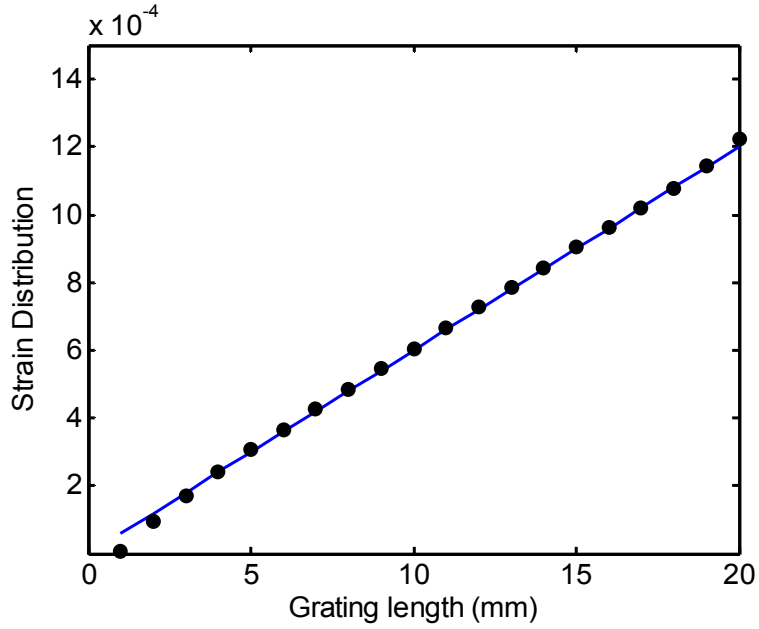
x 10^-4
14
12
10
8
6
4
2
Strain Distribution
0
5
10
15
20
Grating length (mm)

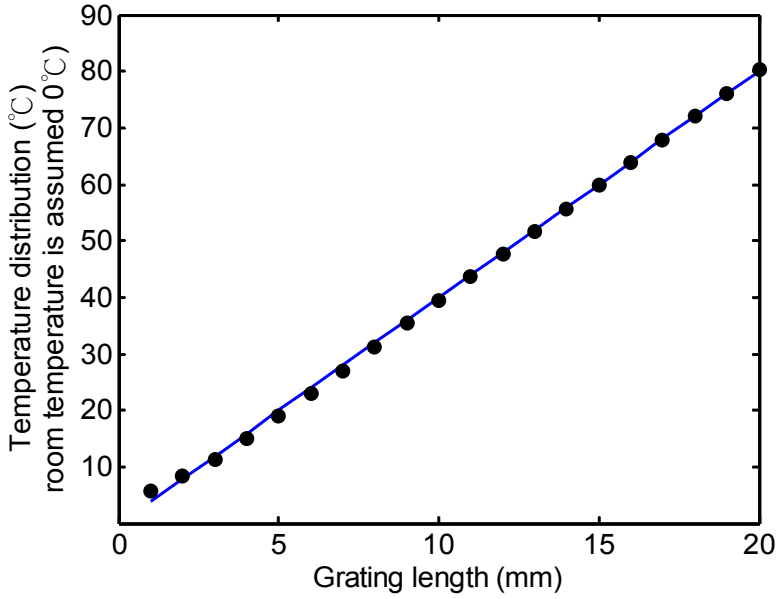
90
80
70
60
50
40
30
20
10
Temperature distribution (℃)
room temperature is assumed 0℃)
0
5
10
15
20
Grating length (mm)

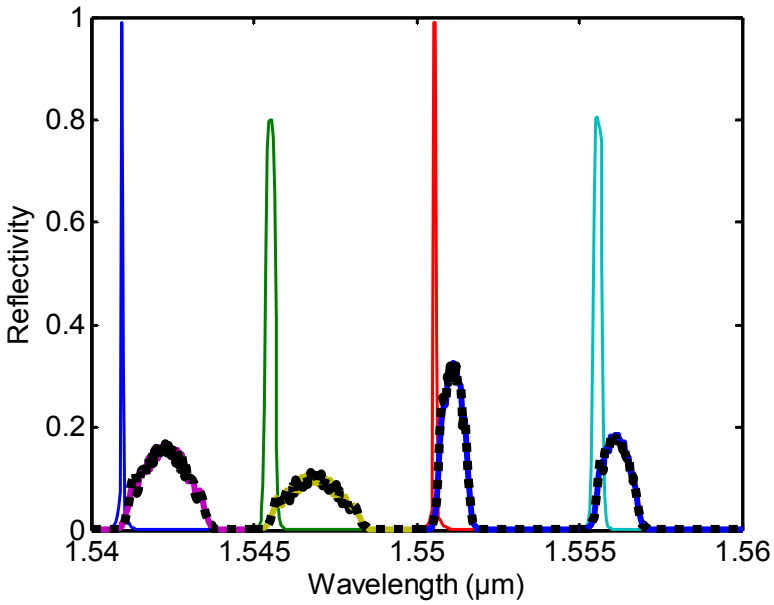

Figure 6(a) The ideal linear positive gradient strain profile (solid line) and reconstructed result (dashed line) with genetic algorithm. (b) The ideal linear positive gradient temperature profile (solid line) and reconstructed result (dashed line) with genetic algorithm. (c) The attenuated four FBG's spectra and four reflection intensity spectra (solid line) under ideal temperature and strain profiles. The reconstructed reflection intensity spectra with optimal temperature and strain profiles (dashed line).

Figs. 7(a) and 7(b) show linear positive gradient strain and negative gradient temperature distribution profiles, respectively. These strain and temperature profiles generate the four reflective spectra shown in Fig. 7(c). In Figs. 7(a) and 7(b), it is obvious that the strain and temperature profiles (dotted lines) reconstructed using the genetic algorithm are in good agreement with the ideal strain and temperature profiles (solid curves). Moreover, the setting attenuation factors are Att.1=0.8 Att.2=0.4, Att.3=0.7, Att.4=0.8 and reconstructed attenuation factors are Att.1=0.7913 Att.2=0.4027, Att.3=0.6983, and Att.4=0.4979.

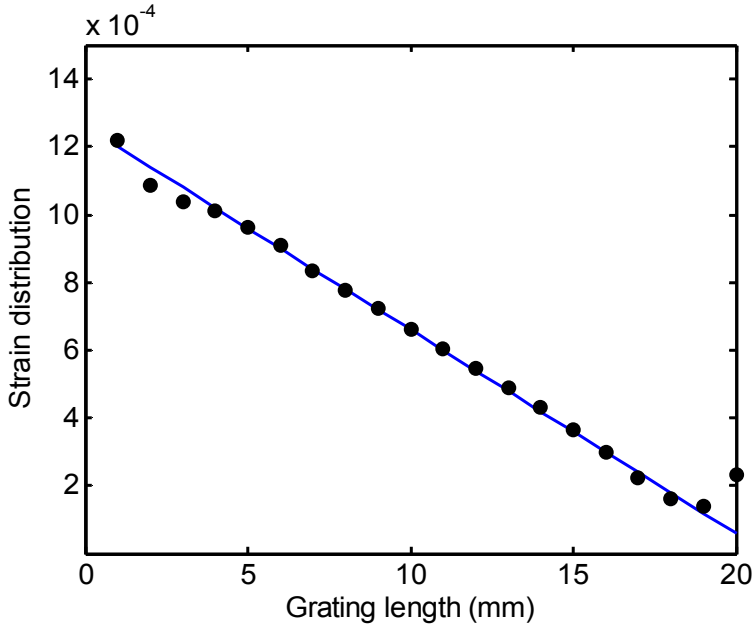

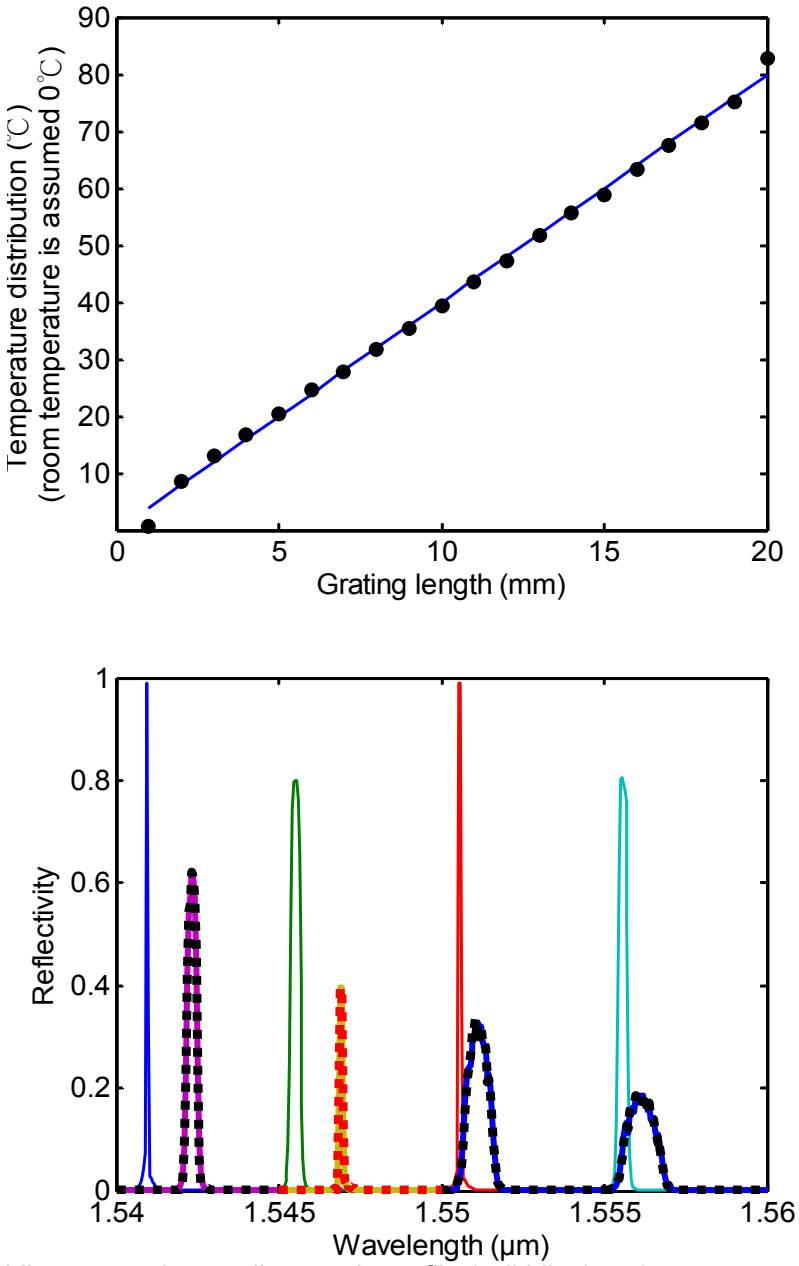

Figure 6(a) The ideal linear negative gradient strain profile (solid line) and reconstructed result (dashed line) with genetic algorithm. (b) The ideal linear positive gradient temperature profile (solid line) and reconstructed result (dashed line) with genetic algorithm. (c) The attenuated four FBG's spectra and four reflection intensity spectra (solid line) under ideal temperature and strain profiles. The reconstructed reflection intensity spectra with optimal temperature and strain profiles (dashed line).

Finally, the proposed scheme was used to simulate the complicated strain and linear positive gradient temperature distribution profiles shown in Figs. 7(a) and 7(b), respectively. Traditional inverse algorithms such as the Fourier technique fail to provide accurate results for these non-continuous strain and temperature distributions [3]. However, as shown in Figs. 7(a) and 7(b), the reconstructed strain and temperature profiles (dotted curves) obtained using the proposed scheme are in good agreement with the original profiles. Moreover, in Fig. 7(c), a good agreement is found between the attenuated reflection intensity spectra under the ideal strain and temperature distributions and the reconstructed reflection intensity spectra based on the calculated temperature and strain distribution profiles. Also, the setting attenuation factors are Att.1=0.8, Att.2=0.4, Att.3=0.7, Att.4=0.5 and reconstructed attenuation factors are Att.1=0.7939, Att.2=0.3966, Att.3=0.6817, and Att.4=0.5000.

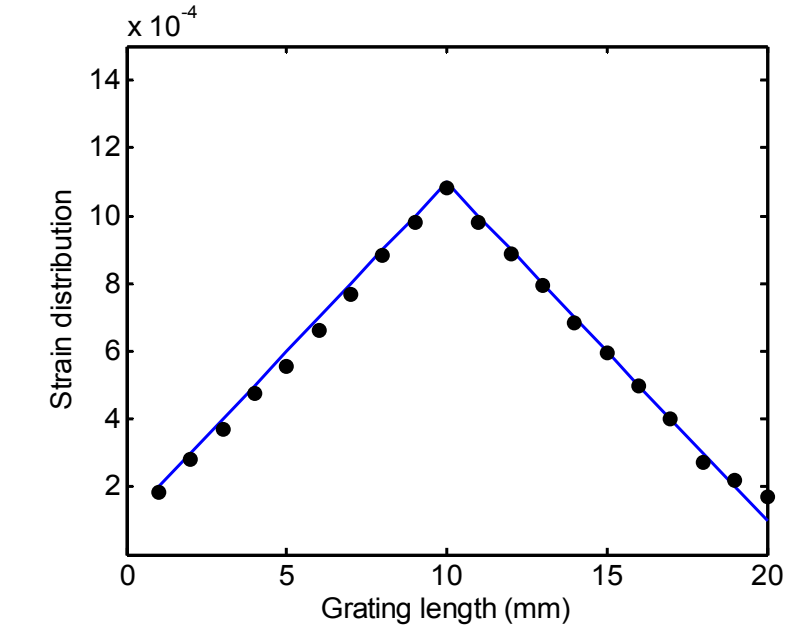
x 10^-4
14
12
10
8
6
4
2
Strain distribution
0
5
10
15
20
Grating length (mm)

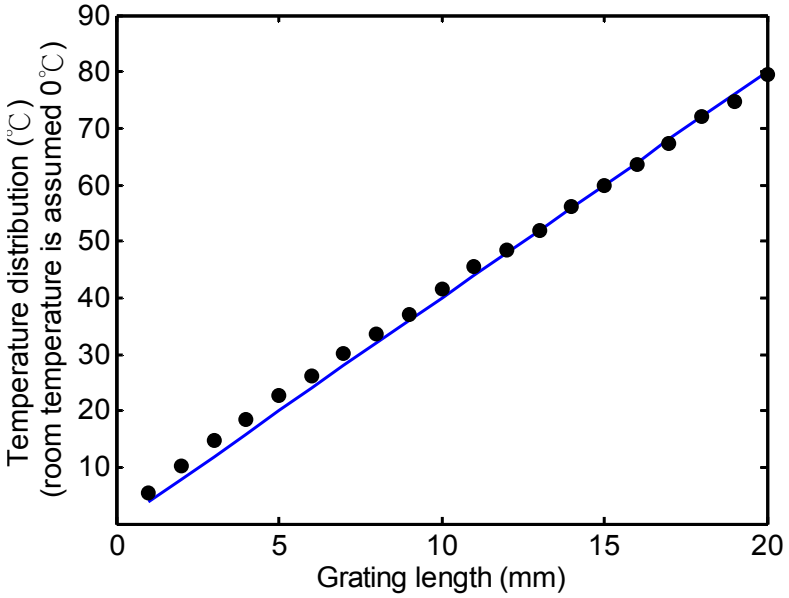
90
80
70
60
50
40
30
20
10
Temperature distribution (℃)
(room temperature is assumed 0℃)
0
5
10
15
20
Grating length (mm)

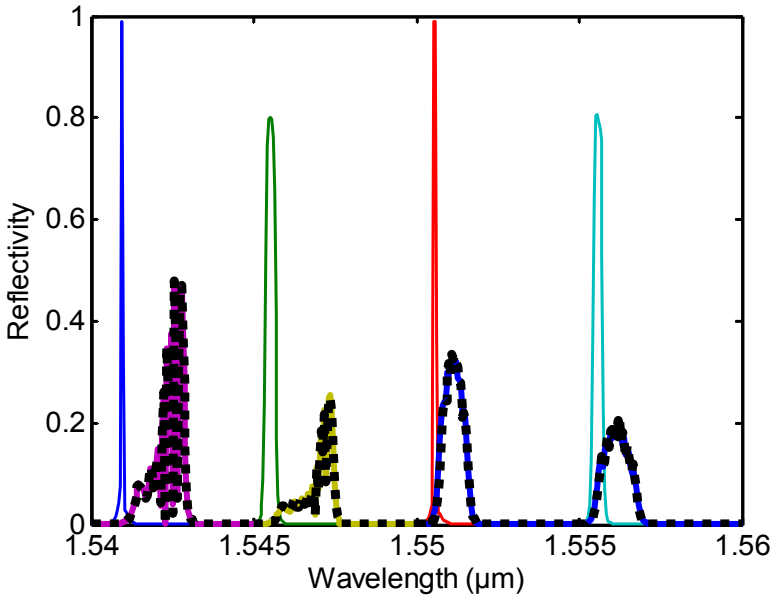
1
0.8
0.6
0.4
0.2
0
Reflectivity
1.54
1.545
1.55
1.555
1.56
Wavelength (μm)

Figure 9(a) The ideal complex strain profile (solid line) and reconstructed result (dashed line) with genetic algorithm. (b) The ideal linear positive gradient temperature profile (solid line) and reconstructed result (dashed line) with genetic algorithm. (c) The attenuated four FBG's spectra and four reflection intensity spectra (solid line) under ideal temperature and strain profiles. The reconstructed reflection intensity spectra with optimal temperature and strain profiles (dashed line).

4. Conclusions

This article has presented a novel arbitrary strain and temperature distribution sensing approach using a genetic algorithm for the inverse tracking of four FBG intensity spectra. The effectiveness and feasibility of the proposed approach have been demonstrated by solving the inverse problem of strain and temperature profile sensing. The simulation results have shown that the genetic algorithm provides an effective means of optimally establishing the solution of a complicated strain and temperature system. Also, the current method adds the attenuation power ration into the genetic algorithm. It makes this arbitrary strain and temperature distribution sensing method more completely and can be used in the practical applications.

References

[1] M. Volanthen, H. Geiger, M. J. Cole, and J. P. Dakin, "Measurement of arbitrary strain profiles within fibre gratings," Electron. Lett., vol.32, pp. 1028-1029, 1996.

[2] C. J. S. de Matos, P. Torres, L. C. G. Valente, W. Margulis, and R. Stubbe, "FBG characterization and shaping by local pressure," J. Lightwave Technol., vol.19, pp. 1206-1211, 2001.

[3] N. Roussel, S. Magne, C. Martinez, and P. Ferdinand, "Measurement of index modulation along fiber Brgg gratings by side scattering and local heating techniques," Optical Fiber Techno., vol. 5, pp. 119-132, 1999.

[4] J. Azana, M.A. Muriel, L.R. Chen, and P.W.E. Smith, "FBG period reconstruction using time-frequency signal analysis and application to distributed sensing," J. Lightwave Technol., vol.19, pp. 646-654, 2001.

[5] R. Feced, M. N. Zervas, and M. A. Muriel, "An efficient inverse scattering algorithm for the design of nonuniform FBGs," J. Quantum Electron, vol. 35, pp. 1105-1115, 1999.

[6] J. Skaar and K. M. Risvik, "A genetic algorithm for the inverse problem in synthesis of fiber gratings," J. Lightwave Technol., vol.16, pp. 1928-1932, 1998.

[7] G. Cormier and R. Boudreau, "Real-coded genetic algorithm for Bragg grating parameter synthesis," J.Opt. Soc. Am. B., vol.18, pp. 1771-1776, 2001.

[8] P. Dong, J. Azana, A. G. Kirk, "Synthesis of FBG parameters from reflectivity by means of a simulated annealing algorithm." Optics Comm., vol. 228, pp. 303-308, 2003.

[9] S. Huang, M. M. Ohn, and R. M. Measures, "Continuous arbitrary strain profile measurements with FBGs," Smart Mater. Struct., vol. 7, pp. 248-256, 1998.

[10] H. C. Cheng and Y. L. Lo, "The synthesis of multiple parameters of arbitrary FBGs via a genetic algorithm and two thermally-modulated intensity spectra," J. Lightwave Technol., vol. 23, pp. 2158-2168, 2005

[11] J. F. Huang, Y. L. Lo, H. C. Cheng, and S. H. Huang, "Reconstruction of Chirped Fiber Bragg Grating Parameters and Phase Spectrum Using Two Thermally Modulated Intensity Spectra and a Genetic Algorithm" Photo. Techno. Lett., vol. 18, pp. 346-348, 2006

[12] H. C. Cheng and Y. L. Lo, "Arbitrary strain distribution measurement using a genetic algorithm approach and two FBG intensity spectra," Optics Comm., vol. 239, pp. 323-332, 2004.

[13] T. Erdogan, "Fiber grating spectra," J. lightwave Technol., vol.15, pp. 1277-1294, 1997.

[14] Z. Michalewicz, Genetic Algorithms + Data structures = Evolution Programs, New York: Springer-Verlag, 1992.